Research Article

SOHAG JOURNAL OF SCIENCES

https://doi.org/10.21608/sjsci.2024.275575.1185

Molecular Surface Description of Halomethanes and its Relation to Their Physicochemical Properties: A Quantum Chemical Investigation

Ossama Abdeen, Mohamed Ismael, Aly Abdou*

Chemistry Department, Faculty of Science, Sohag University, Sohag 82524, Egypt
**Email: aly_abdou@science.sohag.edu.eg*

Received: 8th March 2024, **Revised:** 2nd May 2024, **Accepted:** 22nd May 2024
Published online: 6th June 2024

Abstract: The relation between a compound's molecular surface and its respective macroscopic properties is a particularly intriguing field of quantitative structure-property relationship (QSPR) studies. More specifically, physicochemical properties like critical volumes Vc and critical pressures Pc are, undoubtedly, amongst the important characteristics for chemical research and chemical industries. Besides, the acentric factor ω has been proven efficacious for a sufficient characterization of fluids. In the present work, we offer a new approach to the determination of the mentioned properties of halomethanes from computed molecular surface properties assisted by a simple atomic contribution. The molecular surfaces of the halomethanes were first studied in terms of their molecular electrostatic potential (MEP) maps and average local ionization energy (ALIE) maps, in addition to their molecular surfaces' areas and volumes. Certain molecular surface properties were calculated and employed as independent variables in a multiple linear regression (MLR) analysis against Vc, Pc and ω. For Vc, MLR based on two variables resulted in a correlation coefficient R = 0.996 and a relative standard error RSE = 2.68%. For Pc, using two additional independent variables, R and RSE were found to be 0.980 and 4.48%. Finally, for ω, using one more independent variable, R and RSE were found to be 0.978 and 5.79%, respectively. This was a quite good improvement of Vc prediction and a very substantial improvement of Pc prediction, compared to results obtained by applying variables from previous literature to the same halomethanes under study. Moreover, the prediction of the acentric factor from quantum-chemical calculation is unprecedented in literature.
Keywords: Molecular surface, Molecular electrostatic potential, Average local ionization energy, Halomethanes, Critical volume, Critical pressure, Acentric factor.

1. Introduction

Critical volumes and pressures, V_c and P_c, respectively, are essential characteristics of fluids upon which phase transition is dependent. Accurate experimental measurement of V_c is usually a troublesome task, because a fluid's volume varies substantially for even very small variations in temperature or pressure near the critical point[1, 2]. In addition to V_c and P_c, the acentric factor ω is demonstrated to be very useful for a sufficient description of a fluid's equation of state[3]. Many methodologies and relationships have been carried out or sought to predict the values of V_c and P_c for different compounds[4-6]. Of these approaches, the prediction of critical constants from pure quantum-chemical calculations is, arguably, the most interesting. The essence of this approach lies in what is known as the general interaction property function (GIPF). The GIPF is, principally, based on two concepts: the molecular surface and the molecular electrostatic potential[7, 8]. Presumably, in the field of computational chemistry, the most employed approach to define a molecular surface is through computing the molecular electron density[9]. The quantum theory can accurately predict the electron density, resulting from the exotic motion of electrons, at any molecular site in the vicinity of the molecule. Computations and experiments revealed that the electron density decays asymptotically as we go further from the molecule[10]. This leads us to the interesting conclusion of a molecular isosurface that is uniquely defined by an isodensityvalue, usually taken to be 0.001 or 0.002 au. The molecular isosurface, therefore, contains the whole molecule, where it has a defined area and encloses a defined volume, i.e., the molecular volume. On the other hand, the molecular electrostatic potential (MEP) at any point within or in the vicinity of a molecule is the net electrostatic potential (EP) of the positive EP resulting from the nuclei of the molecule and the negative EP resulting from its electron cloud[11]. The GIPF basically aspires to establish relationships between the macroscopic properties of compounds and the distribution of EP onto their respective molecular surfaces[8]. More generally, the molecular surface property approach (MSPA) makes use of other functions besides the EP, like the average local ionization energy (ALIE)[12]. The ALIE at a molecular site is the energy necessary to remove an electron from this site. Since many electrons pass through the molecular site with different energies and different contributions, the ALIE uses the average ionization value. The importance of the ALIE function originates from its capacity to be a measure of the local polarizability, where the lower the ALIE at a molecular site is, the more polarizable this site tends to be[13, 14]. That all being said, halogenated compounds constitute interesting cases in the field of MSPA studies. This is, primarily, because while halogens are classically known for being negative (i.e., nucleophilic) groups, MEP maps reveals positive EP regions on the outermost molecular surface of the halogen atom along the σ bond by which the halogen atom is attached[15]. This positive EP

©2024 Sohag University

region, usually termed as σ-hole, has many applications in noncovalent interactions studies[16], medicinal chemistry[17], and supramolecular chemistry[18]. Fluorine, the smallest halogen, is a special case in this regard, because, due to the small size of its atom, it generally either does not exhibit a σ-hole[15] or, in certain chemical environments, it exhibits a relatively small σ-hole, compared to other halogens[19]. Furthermore, the small size of the fluorine atom makes it nonpolarizable or very weakly polarizable, at least compared to the larger halogens[20, 21]. This makes the fluorine atom fundamentally unique among halogens, in terms of both electrostatic properties and polarizability. In the current study, halomethanes are studied from the MSPA point of view. The MEP and ALIE maps are generated and depicted, while EP-derived and ALIE-derived molecular surface descriptors are tabulated. These maps and tables help conceptualize, qualitatively and quantitatively, how far halomethanes are different from, and similar to, each other. To fulfill the purpose of the study, the critical volumes of the halomethanes are correlated with two variables of their molecular surface properties using ALIE, as will be elucidated in the computational methodology section. Moreover, the respective critical pressures are correlated with 4 independent variables using both ALIE and EP to account for polarization and electrostatic intermolecular forces, respectively, in addition to the number of fluorine atoms in the molecule. Finally, the acentric factors are correlated with the same set of independent variables of Cp in addition to a variable representing the number of the hydrogen atoms in the molecule. To our knowledge, this is the first quantum-chemical endeavor to relate acentric factors to molecular surface descriptors.

2. Computational Methodology

2.1. Molecular Surface Analysis

First, halomethanes of known experimental critical pressures and volumes and acentric factors have been optimized at MP2/aug-cc-pVDZ(PP) level of theory via GAMESS-US software [22] implemented in Chemcompute Lab servers [23]. Using the optimized geometries, additional files that contain the molecular wavefunctions' data were generated at the same level of theory using GAMESS-US software. These files have been then used as input files for Multiwfn 3.8 software [24]. Using the Multiwfn software, the molecular surface properties have been computed onto molecular electron-density isosurfaces of value 0.001 au. An optimized code, implemented in Multiwfn software, was employed for the electrostatic potential calculations [25]. The molecular surfaces, mapped with EP and ALIE functions, were visualized via VMD software [26]. The molecular surface was chosen to be of an electron isodensity value of 0.001 au. Molecular surface properties, that have been computed, included molecular surface area *A*, measured in Å^2 and molecular volume V, measured in Å^3. The computed EP-derived properties included minimal, maximal, average positive and average negative electrostatic potential, V_{min}, V_{max}, V^+_{avg} and V^-_{avg}, respectively, measured in kcal/mol. The computed EP-based properties included also positive and negative electrostatic molecular surface areas $A^+$and A^-, respectively. Positive, negative and total electrostatic potential variances, Var^+, Var^-, and Var^{tot}, respectively, have also been computed and the balance parameter $\mu = \frac{Var^+ \times Var^-}{(Var^{tot})^2}$has been calculated to study the correlation obtained from the independent variables in previous literature [7]. The computed ALIE-derived properties included the minimum, maximum and average values of the ALIE ($ALIE_{min}$, $ALIE_{max}$ and $ALIE_{avg}$. respectively) onto the molecular surface, measured in eV. To carry out multiple linear regression (MLR), independent variables, defined below, have been calculated and tabulated against the critical volumes, critical pressures and acentric factors of the studied halomethanes from literature [27, 28].

2.2. Independent Variables

The independent variables, that are used in the multiple linear regression for the prediction of V_c, are defined as follows:

i) Molecular Volume, V, as defined in the introduction,
ii) a variable for polarization interaction, $Z = \frac{A}{ALIE_{avg}}$.
iii) Two more independent variables are used for the prediction of P_c besides the above two, namely:
iv) a variable for electrostatic interaction, $S = (V_{max} - V_{min}) \times (V^+_{avg} - V^-_{avg})$,
v) the number of fluorine atoms in the molecule, N_F.
vi) One last independent variable used for the prediction omega besides the above four, namely:
vii) the number of hydrogen atoms in the molecule, N_H.

3. Results and Discussion:

3.1. Molecular Electrostatic Potentials (MEPs)

For the halomethanes, MEPs were generated and plotted onto molecular surfaces of electron isodensity values of 0.001 au and visualized in Figures 1 and S1 by means of VMD software. The MEPs are visualized in an RGB color scale ranging from –0.01 au (red) to +0.01 au (blue). Moreover, V_{min}, V_{max}, V^+_{avg}, V^-_{avg}, A^+, A^-, Var^+ and $Var^-$of the halomethanes were extracted and tabulated in Table S1.

As seen in Figures 1 and S1, the hydrogen atoms generally carry positive electrostatic regions while the fluorine atoms generally do not carry a significant positive electrostaticregion, basically due to the small size of the fluorine atom. For the other halogens, Cl, Br and I, it is found that when the central carbon atom is attached to an electron-withdrawing group, they clearly exhibit their positive electrostatic σ-holes on the outermost molecular surface along the C-X bond, where X = Cl, Br or I. A conclusive example is seen in Figure 1, when comparing CH_3Cl, CH_3Br and CH_3I molecules on one hand, and CF_3Cl, CF_3Br and CF_3I molecules on the other hand. First, it is clear that the hydrogen and fluorine atoms carry positive and negative electrostatic potentials, respectively. Second, the effect of the electron-withdrawing F_3 atoms is pronounced in the larger positive σ-holes carried by the Cl, Br and I atoms in the CF_3Cl, CF_3Br and CF_3I molecules, respectively, compared to the CH_3Cl CH_3Br and CH_3I molecules, respectively. The effect of gradual incorporation of halogen atoms is further illuminated in Figure S2. In FigureS2, the MEPs of CH_nF_{4-n} molecules (where $0 \le n \le 4$) are put alongside each other for the sake of visual comparison. It is obvious that increasing the number of F atoms, which are electron-withdrawing groups, increases not only the positivity

of the hydrogen atom(s), but also causes the central carbon atom to carry positive EP regions, which are fully manifested in a positive EP belt in CF_4 molecule.

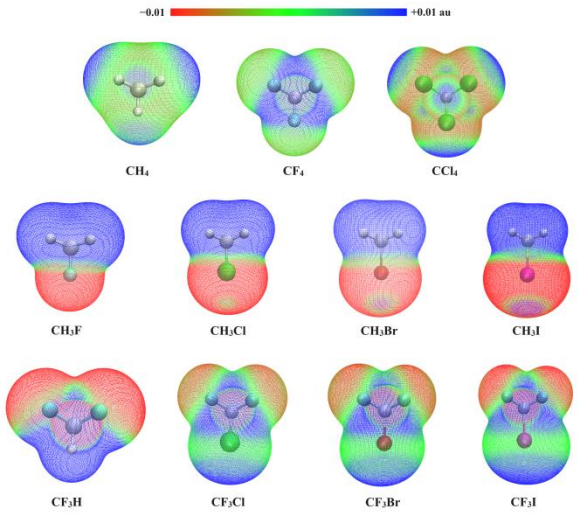

Figure 1: Molecular electrostatic potentials (MEPs) of some halomethanes mapped onto molecular surfaces of electron isodensity values of 0.01 au. The RGB color scale ranges from −0.01 au (red) to +0.01 au (blue)

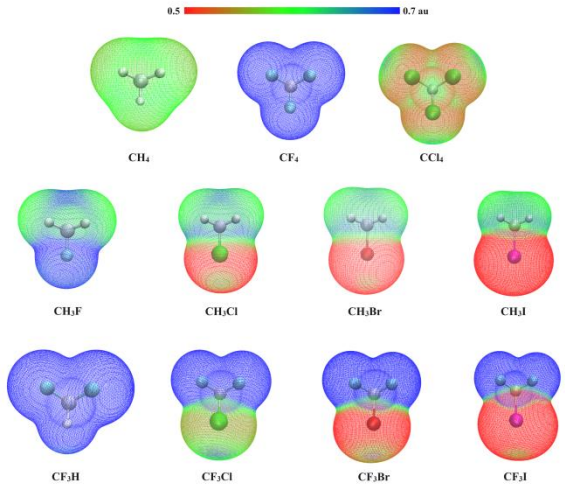

Figure 2: The average local ionization energy (ALIE) maps of some halomethanes onto molecular surfaces of electron isodensity values of 0.01 au. The RGB color scale ranges from 0.5 au (red) to 0.7 au (blue)

3.2. Average Local Ionization Energy (ALIE) Maps

The halomethanes under study, the ALIE was calculated and mapped onto electron isodensitysurfaces of 0.001 au value and visualized in Figures **2** and **S3** via VMD software. The RGB color scale was taken from 0.5 au (red) to 0.7 au (blue). Additionally, $ALIE_{min}$, $ALIE_{max}$ and $ALIE_{avg}$ values were tabulated in Table **S1.** The minimum and maximum ALIE values, tabulated in Table S1 and measured in eV, quantitatively show the exact range of ALIE on the molecular surface. For example, CF_4 has an $ALIE_{min}$ and $ALIE_{max}$of values 21.4 eV (0.786 au) and 23.96 eV (0.881 au), respectively, on its molecular surface, while CH_3I has $ALIE_{min}$ and $ALIE_{max}$ values of 10.63 eV (0.391 au) and 18.06 eV (0.664 au), respectively.From **Figures 2** and **S3**, it is obvious that, generally, the larger a halogen atom is, the more region with a lower ALIE value (i.e., red color) it bears. Taken the ALIE as a measure of polarizability, it is found that the hydrogen atom is generally more polarizable than the fluorine, whichis also the least polarizable atom among halogens. Moreover, when electron-withdrawing groups are attached to the central carbon atom, the halogen atom (i.e., Cl, Br orI) becomes relatively less polarizable i.e., with a smaller red region of low ALIE. For example, in Figure 2, whencomparing the X atom in CH_3XandCF_3X molecules,where X is Cl, Br and I, it is found that the X atom carries a larger area of a low ALIE in CH_3X than it does in CF_3X molecules. Using chemical intuition, it can be inferred that the electron-withdrawing effect of the F_3 atoms makes the electrons more tied to the X atom and, consequently, increases the ALIE on the X atom's molecular surface. It is also obvious that the fluorine atom seems to lack efficient polarizable regions, at least compared to the other halogens. Bearing in mind that the fluorine atom also lacks an effective σ-hole, in general, this makes fluorine fundamentally distinct from other halogens, as previously noted.

3.3. Multiple Linear Regression and the Prediction of Critical Constants

As shown in Table **1**, for the halomethanes under study, experimental critical volumes and pressures, and acentric factors, V_c, P_c, and ω, respectively, were tabulated against the computed molecular descriptors defined in the computational methodology section, namely, V, Z, S, N_F and N_H.

In previous literature, V_c was correlated against the molecular surface area *A* for sets of compounds in the form $V_c = \alpha A^n + \beta$, where n differs from a set of compounds to another[7]. Choosing n = 1 for the halomethanes under study, an excellent correlation coefficient R = 0.987 and a relative standard error RSE = 4.53% were obtained. Using molecular volume V and the polarization variable Z, defined in the computational methodology section, R improved to 0.996 and RSE decreased to 2.68%. This was a reasonable improvement towards a more accurate prediction. The improvement was very clearly pronounced in the case of P_c. In previous literature, P_c was defined for a set of compounds in terms of the molecular surface area *A* and the variable $\frac{\mu \times Var^{tot}}{A}$[7].When these two variables were applied for linear regression against the critical pressures of the halomethanes, a drastically poor correlation (R = 0.546, RSE = 18.03%) was obtained. This presumably due to the existence of large, and highly polarizable, atoms like Bromine and Iodine in the halomethanesunder study. Likewise, the existence of the highly polarizing fluorine atoms may have exacerbated the situation making the intermolecular forces far more complicated beyond simple electrostatics.

When a multiple linear regression (MLR) was performed between the reciprocals of the halomethanes' critical pressures ($1/P_c$) and the independent variables V, Z, S and N_F defined in the computational methodology section, a far better correlation

(R = 0.980, RSE = 4.48%) was obtained. For the acentric factor ω, where the independent variables V, Z, S, N_F and N_H were used, A very good correlation (R = 0.978, RSE = 5.79%) was obtained. Table 2 concludes the correlation results of the MLR analysis carried out for the halomethanes, including the correlation parameters R and RSE and the coefficients of the independent variables and their respective p-values. It is noticed that all the p-values of the independent variables have values far less than 0.05, indicating their statistical significance. The experimental (X-axis) versus predicted (Y-axis) values of V_c, $1/P_c$ and ω are depicted in Figure 3.

Table 1: Halomethanes' critical volumes (Vc), critical pressures (Pc) and acentric factors (ω) tabulated against their respective molecular properties employed in the multiple linear regression, as outlined in the computational methodology section

Halomethane	V_c(mL/mol)	P_c (Mpa)	ω	V (Å^3)	Z (Å^2/eV)	S (kcal/mol)^2	N_F	N_H
CCl_3Br	287.35	4.980	0.190	136.64	9.56	348.89	0	0
CCl_4	275.67	4.550	0.193	129.41	8.91	267.82	0	0
CF_2Br_2	246.84	4.450	0.180	110.11	7.64	404.55	2	0
CF_2Cl_2	215.92	4.100	0.178	95.47	6.35	301.63	2	0
CF_2ClBr	236.23	4.220	0.177	102.79	6.99	382.92	2	0
CF_3Br	198.55	3.970	0.173	85.21	5.62	382.27	3	0
CF_3Cl	171.24	3.890	0.178	77.86	5.01	303.99	3	0
CF_3I	227.80	3.860	0.180	98.45	6.68	542.62	3	0
CF_4	139.69	3.740	0.177	59.99	3.69	316.36	4	0
$CFCl_3$	245.30	4.408	0.187	112.65	7.66	313.86	1	0
CH_2Br_2	204.51	6.950	0.200	101.45	8.11	925.51	0	2
CH_2Cl_2	178.81	6.420	0.214	86.56	6.65	1,052.71	0	2
CH_2ClBr	187.51	6.670	0.218	94.01	7.37	989.12	0	2
CH_2F_2	120.98	5.780	0.277	50.06	3.59	1,892.80	2	2
CH_2FCl	152.17	5.700	0.210	68.52	5.11	1,483.64	2	2
CH_2I_2	248.00	6.800	0.220	127.90	10.62	783.93	0	2
CH_3Br	150.70	6.850	0.150	71.79	5.99	933.49	0	3
CH_3Cl	138.32	6.710	0.153	64.16	5.24	1,015.45	0	3
CH_3F	109.78	5.880	0.197	45.61	3.60	1,749.34	1	3
CH_3I	175.23	6.700	0.150	85.21	7.27	814.20	0	3
CH_4	98.60	4.599	0.012	41.89	3.73	61.83	0	4
$CHBr_3$	266.03	6.200	0.190	130.34	9.96	711.14	0	1
$CHCl_3$	229.57	5.400	0.212	108.44	7.89	752.15	0	1
CHF_2Cl	164.70	4.988	0.221	73.16	5.05	1,216.43	2	1
CHF_3	132.10	4.800	0.263	54.94	3.63	1,628.44	3	1
$CHFCl_2$	196.04	5.183	0.208	90.99	6.48	998.57	1	1

Table 2: Correlation coefficients (R), relative standard errors (RSE), the coefficients of the independent variables (Coeff) and the p-values of the independent variables of the multiple linear regression (MLR) of molecular properties against both critical volumes (Vc), the reciprocals of critical pressures (1/Pc) and the acentric factors (ω)

Parameter	V_c		$1/P_c$		ω	
R	0.996		0.980		0.978	
RSE	2.68%		4.48%		5.79%	
Variable	Coeff	p-value	Coeff	p-value	Coeff	p-value
V	2.93	4.43×10^{-17}	0.002	8.32×10^{-06}	−0.008	2.29×10^{-04}
Z	−14.03	4.56×10^{-08}	−0.031	4.62×10^{-06}	0.093	1.10×10^{-04}
S			-4.1×10^{-05}	3.13×10^{-09}	9.87×10^{-05}	3.60×10^{-14}
N_F			0.012	4.65×10^{-05}	−0.026	1.17×10^{-03}
N_H					−0.099	5.96×10^{-06}
Constant	23.23		0.234		0.402	

©2024 Sohag University

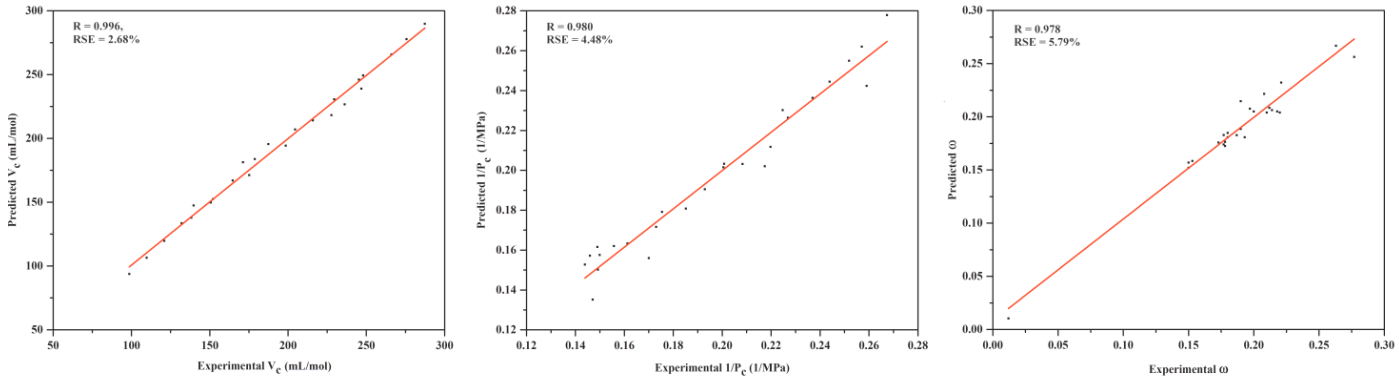

Figure 3: Experimental (X-axis) versus predicted (Y-axis) values of the critical volumes (Vc), critical pressures (Pc) and acentric factors (ω) of the studied halomethanes with the correlation coefficients (R) and relative standard errors (RSE) depicted

4. Conclusion

In the present work, we established a methodology to calculate critical volumes and pressures of halomethanes from pure quantum chemical calculations assisted by a simple atomic contribution. First, molecular surface properties of the halomethanes were discussed in light of their electrostatic potential and average local ionization energy maps. The fluorine atom was seen to have a fundamentally different nature from the other halogens as it carried no conspicuous electrophilic positive electrostatic region (a σ-hole), nor did it have an efficient polarizability manifested in the ALIE map onto its atomic surface. The effect of the chemical environment was also shown determinant regarding the properties of the halogen atom X, where X = Cl, Br and I. It was seen that the electrostatically positive regions carried by the halogen atoms increased in size and magnitude when the X atom was attached to stronger electron-withdrawing groups. Moreover, the ALIE on the atomic surface was shown to increase (making the atom less polarizable) when the central carbon atom was attached to stronger electron-withdrawing groups. Using multiple linear regression (MLR), we could draw a relationship between the molecular surface characteristics as independent variables and the respective critical volumes Vc, reciprocals of the critical pressures 1/Pc and acentric factors ω with R values of 0.996, 0.980 and 0.978, respectively, and RSE values of 2.68%, 4.48% and 5.79%, respectively. Our results constitute a significant improvement to previous literature, a successful attempt to predict new physicochemical properties and a step forward towards more profound and detailed insights into the general subject of the molecular surface property approach (MSPA).

CRediT authorship contribution statement:

Conceptualization, O. Abdeen, M. Ismael, A. Abdou; methodology, O. Abdeen, M. Ismael, A. Abdou; software, O. Abdeen, M. Ismael, A. Abdou; validation, O. Abdeen, M. Ismael, A. Abdou; formal analysis, O. Abdeen, M. Ismael, A. Abdou; investigation, O. Abdeen, M. Ismael, A. Abdou; resources, O. Abdeen, M. Ismael, A. Abdou; data curation, O. Abdeen, M. Ismael, A. Abdou; writing—original draft preparation, O. Abdeen, M. Ismael, A. Abdou; writing—review and editing, O. Abdeen, M. Ismael, A. Abdou; visualization, O. Abdeen, M. Ismael, A. Abdou; supervision, M. Ismael, A. Abdou; project administration, M. Ismael, A. Abdou; All authors have read and agreed to the published version of the manuscript."

Data availability statement

The data used to support the findings of this study are available from the corresponding author upon request.

Declaration of competing interest

The authors declare that they have no known competing financial interests or personal relationships that could have appeared to influence the work reported in this paper.

References

[1] S.J.B.S.S.P. Pickering, *Scientific Papers of the Bureau of Standards*21(541) (1926) 597-629.
[2] M.A. Martínez-Vitela, J. Gracia-Fadrique, *Ingeniería y Ciencia* 15 (2019) 81-99.
[3] K. S.Pitzer, *ACS Symposium Series* 133, (1980) 1-10.
[4] A. Vetere, *Fluid Phase Equilib*. 109(1) (1995) 17-27.
[5] A.R. Katritzky, M. Kuanar, S. Slavov, C.D. Hall, M. Karelson, I. Kahn, D.A. Dobchev, *Chem. Rev*. 110(10) (2010) 5714-5789.
[6] J.O. Valderrama, P.A. Robles, *Ind. Eng. Chem. Res*. 46(4) (2007) 1338-1344.
[7] J.S. Murray, P. Lane, T. Brinck, K. Paulsen, M.E. Grice, P. Politzer, *The Journal of Physical Chemistry* 97(37) (1993) 9369-9373.
[8] J.S. Murray, T. Brinck, P. Lane, K. Paulsen, P. Politzer, *Journal of Molecular Structure: THEOCHEM* 307 (1994) 55-64.
[9] R.R. Gabdoulline, R.C. Wade, *J. Mol. Graphics* 14(6) (1996) 341-353.
[10] C.F. Matta, R.J. Gillespie, *J. Chem. Educ*. 79(9) (2002) 1141.
[11] J.S. Murray, P. Politzer, *WIREs Computational Molecular Science* 1(2) (2011) 153-163.
[12] T. Brinck, J.H. Stenlid, *Advanced Theory and Simulations* 2(1) (2019) 1800149.
[13] P. Politzer, J. S. Murray. *Theoretical and Computational Chemistry* 19 (2007) 119-137.
[14] P. Politzer, J.S. Murray, F.A. Bulat, *J. Mol. Model.* 16(11) (2010) 1731-1742.
[15] P. Politzer, J.S. Murray, T. Clark, *PCCP* 15(27) (2013) 11178-11189.
[16] I. Alkorta, J. Elguero, A.J.C. Frontera, *Crystals* 10(3) (2020) 180.
[17] Á.M. Montaña, *ChemistrySelect* 2(28) (2017) 9094-9112.
[18] J.Y.C. Lim, P.D. Beer, *Chem* 4(4) (2018) 731-783.

[19] A. Varadwaj, P.R. Varadwaj, B.-Y. Jin, *Int. J. Quantum Chem* 115(7) (2015) 453-470.
[20] J.S. Murray, P.G. Seybold, P. Politzer, *JChTh* 156 (2021) 106382.
[21] D. Chopra, *Crystal Growth & Design* 12(2) (2012) 541-546.
[22] G.M.J. Barca, C. Bertoni, L. Carrington, D. Datta, N. De Silva, J.E. Deustua, D.G. Fedorov, J.R. Gour, A.O. Gunina, E. Guidez, T. Harville, S. Irle, J. Ivanic, K. Kowalski, S.S. Leang, H. Li, W. Li, J.J. Lutz, I. Magoulas, J. Mato, V. Mironov, H. Nakata, B.Q. Pham, P. Piecuch, D. Poole, S.R. Pruitt, A.P. Rendell, L.B. Roskop, K. Ruedenberg, T. Sattasathuchana, M.W. Schmidt, J. Shen, L. Slipchenko, M. Sosonkina, V. Sundriyal, A. Tiwari, J.L. Galvez Vallejo, B. Westheimer, M. Włoch, P. Xu, F. Zahariev, M.S. Gordon, *The Journal of Chemical Physics* 152(15) (2020) 154102.
[23] M.J. Perri, S.H. Weber, *J. Chem. Educ*. 91(12) (2014) 2206-2208.
[24] T. Lu, F. Chen, *J. Comput. Chem.* 33(5) (2012) 580-592.
[25] J. Zhang, T. Lu, *PCCP* 23(36) (2021) 20323-20328.
[26] W. Humphrey, A. Dalke, K. Schulten, *J. Mol. Graphics* 14(1) (1996) 33-38.
[27] C.L. Yaws, P.K. Narasimhan, *William Andrew Publishing, Norwich, NY,* (2009) 1-95.
[28] H.W. Xiang, J. Phys. *Chem. Ref. Data* 30(5) (2001) 1161-1197.